# Intelligent Gait Analysis and Evaluation System Based on Cane Robot

Qingyang Yan, *Student Member, IEEE*, Jian Huang, *Senior Member, IEEE*, Dongrui Wu, *Senior Member, IEEE*, Zhaohui Yang, Yujie Wang, Yasuhisa Hasegawa, *Member, IEEE*, and Toshio Fukuda, *Life Fellow, IEEE*

***Abstract*— Gait analysis and evaluation are vital for disease diagnosis and rehabilitation. Current gait analysis technologies require wearable devices or high-resolution vision systems within a limited usage space. To facilitate gait analysis and quantitative walking-ability evaluation in daily environments without using wearable devices, a mobile gait analysis and evaluation system is proposed based on a cane robot. Two laser range finders (LRFs) are mounted to obtain the leg motion data. An effective high-dimensional Takagi-Sugeno-Kang (HTSK) fuzzy system, which is suitable for high-dimensional data by solving the saturation problem caused by softmax function in defuzzification, is proposed to recognize the walking states using only the motion data acquired from LRFs. The gait spatial-temporal parameters are then extracted based on the gait cycle segmented by different walking states. Besides, a quantitative walking-ability evaluation index is proposed in terms of the conventional Tinetti scale. The plantar pressure sensing system records the walking states to label training data sets. Experiments were conducted with seven healthy subjects and four patients. Compared with five classical classification algorithms, the proposed method achieves the average accuracy rate of 96.57%, which is improved more than 10%, compared with conventional Takagi-Sugeno-Kang (TSK) fuzzy system. Compared with the gait parameters extracted by the motion capture system OptiTrack, the average errors of step length and gait cycle are only 0.02 m and 1.23 s, respectively. The comparison between the evaluation results of the robot system and the scores given by the physician also validates that the proposed method can effectively evaluate the walking ability.**

***Index Terms*— Cane robot, gait analysis, walking-ability evaluation, machine learning.**

Manuscript received 17 November 2021; revised 29 July 2022; accepted 11 September 2022. Date of publication 13 October 2022; date of current version 24 October 2022. This work was supported in part by the International Science and Technology Cooperation Program of China under Grant 2017YFE0128300 and in part by the International Cooperation Key Program of Hubei Province under Grant 2021EHB003. *(Corresponding authors: Jian Huang; Zhaohui Yang.)*

This work involved human subjects in its research. Approval of all ethical and experimental procedures and protocols was granted by Tongji Medical College, Huazhong University of Science and Technology, under IORG No: IORG0003571, and performed in line with the Declaration of Helsinki.

Qingyang Yan, Jian Huang, and Dongrui Wu are with the Key Laboratory of Ministry of Education for Image Processing and Intelligent Control, School of Artificial Intelligence and Automation, Huazhong University of Science and Technology, Wuhan, Hubei 430074, China (e-mail: yanqingyang@hust.edu.cn; huang_jan@mail.hust.edu.cn; drwu@hust.edu.cn).

Zhaohui Yang and Yujie Wang are with the Department of Rehabilitation Medicine, Union Hospital, Tongji Medical College, Huazhong University of Science and Technology, Wuhan 430022, China (e-mail: annyhao430@163.com; fernweh@hust.edu.cn).

Yasuhisa Hasegawa is with the Department of Micro-Nano Systems Engineering, Nagoya University, Nagoya 464-8603, Japan (e-mail: hasegawa@mein.nagoya-u.ac.jp).

Toshio Fukuda is with the Institutes of Innovation for Future Society, Nagoya University, Nagoya 464-8601, Japan (e-mail: tofukuda@nifty.com).

This article has supplementary downloadable material available at https://doi.org/10.1109/TNSRE.2022.3213823, provided by the authors.

Digital Object Identifier 10.1109/TNSRE.2022.3213823

## NOMENCLATURE

| | |
|---|---|
| $P_{ri}, P_{li}, i = 0, 1, 2$ | Feature points of shanks and feet. |
| $P_h$ | The point denoting the user's position in the world coordinate system. |
| $\mathbf{q}_h, \dot{\mathbf{q}}_h, \ddot{\mathbf{q}}_h$ | The user's posture, speed and acceleration. |
| $\mathbf{x}, \dot{\mathbf{x}}, \ddot{\mathbf{x}}$ | The positions, the corresponding velocities and accelerations of both legs and the target human. |
| $\alpha_{lx}, \alpha_{rx}, \alpha_{ly}, \alpha_{ry}$ | Angles of the shanks in the sagittal and coronal planes. |
| $\dot{\alpha}_{lx}, \dot{\alpha}_{ly}, \dot{\alpha}_{rx}, \dot{\alpha}_{ry}$ | Angular velocities of the shanks in the sagittal and coronal planes. |
| $d, \dot{d}$ | Distance and the gradient of the distance between the shanks. |
| $\mathbf{D}$ | The fixed relative posture between the cane robot and the user. |
| $\mathcal{H}, \mathcal{H}_S$ | Original and $Z$-score standardized motion data set, respectively. |
| $\mathcal{M}, \mathcal{M}_T$ | Gait data set and training data set of gait data, respectively. |
| $I_{r,m}$ | Membership degree function for the $m$th attributes after fuzzed in the $r$th rule. |
| $O_j$ | Output of $j$th layer of HTSK fuzzy system. |
| $S_0$ | Static State. |
| $S_1$ | Swing phase of the left leg from $t_{s41}$ till $t_{s12}$. |
| $S_2$ | Double support phase from $t_{s12}$ till $t_{s23}$, when the center of gravity shifts from righ to left. |
| $\omega_r, \bar{\omega}_r, \bar{\omega}_r^*$ | Conventional firing level, normalized firing level, and the improved firing level of HTSK fuzzy system. |

| | |
|---|---|
| $T_l$, $T_r$ | Step time of the left and right leg. |
| $P_{LS}$,$P_{RS}$ | Ratios of the left leg swing phase, and the right leg swing phase. |
| $P_{LD}$, $P_{RD}$ | Double support phases when the center of gravity shifts from right to left, and from left to right, respectively. |
| $v$ | The user's walking speed. |
| $L_l$, $L_r$ | Step lengths of the left leg and right leg. |
| $L_s$, $L_w$ | Stride lengths and step widths of the user. |
| $SI$ | Walking symmetry index of step lengths. |
| $\mathbf{u}$ | The vector of gait paparmeters. |
| $x_{l2}^{t_{s34}}(j)$, $x_{r2}^{t_{s34}}(j)$ | Locations of the left and right legs at $t_{s34}$ of the $j$th gait cycle. |
| $x_{l2}^{t_{s12}}(j)$, $x_{r2}^{t_{s12}}(j)$ | Locations of the left and right legs at $t_{s12}$ of the $j$th gait cycle. |
| std($v$) | Standard deviation of the speed $v$. |
| $I$ | Walking-ability evaluation index. |
| atan2 | Four-quadrant inverse tangent function in the range of $[-\pi, \pi]$. |

## I. Introduction

GAIT analysis and walking-ability evaluation are essential for clinical disease diagnosis and treatment in rehabilitation medicine [1]. Conventional clinical gait analysis and walking-ability evaluation rely on the physician's observation and evaluation of the patients' motion based on clinical scales, such as the Tinetti scale [2] and the Holden functional ambulation scale [3], and so on. Recent developments in sensors and intelligent diagnosis technologies have led to an increasing interest in automatic gait analysis. The intelligent gait analysis system can provide more detailed spatial-temporal parameters including strides, cadences, and walking velocities for evaluating the movement function of the elderly and patients with gait disorders more quickly and accurately than the visual inspection [4], [5], thus benefits the diagnosis and walking-ability evaluation.

Tracking human motion during walking and gait event detection are key technologies in gait analysis. Advanced tools have been applied to obtain motion data. The vision-based motion capture systems with reflective markers are employed due to the high accuracy and low latency [6]. Kinect or other camera devices fixed in the environment are also used to obtain motion data [7]. Wearable systems based on inertial measurement units (IMUs) are used to extract gait parameters, including the speed, gait cycle, and stride length [8], [9], [10]. Plantar pressure measurement systems are alternative widely-applied tools for gait analysis [11], [12]. The plantar pressure sensor can directly detect gait events such as heel strike (HS) and toe off (TO), allowing gait analysis conceivable.

It should be noted that the existing gait analysis technologies are normally limited by the requirement for wearable sensors and the constrained usage space. The high-resolution vision-based motion capture systems (e.g. Vicon, OptiTrack, PTI, etc.) are inconvenient to monitor human motion in personal daily walking environment due to their high cost and usage space limitation. It is also challenging for conventional vision sensors (including Kinect and many commercially available cameras) to attain continuous stable human motion tracking in the daily walking environment due to field angle and ambient light limitations, which makes gait analysis problematic. The plantar force systems are difficult to fit different users, as the number of in-shoe force sensors required varies according to foot size [13].

Among the research of non-wearable gait analysis systems, owing to the high mobility of the mobile robot and combination of vision-based gait detection systems, the gait analysis system based on a mobile robot and vision sensors has become a hot topic over recent years. Chi et al. [14] proposed a gait recognition method by extracting ankle future points based on Kinect and a Turtle-Bot. Paulo et al. [15] proposed a gait analysis method by using the smart walker with detecting feet based on a camera. Since current mobile robot related gait researches depends largely on the above-mentioned vision sensors, there still remain the deficiencies of current gait analysis technologies, such as high-cost, ambient light limitations, multifarious image processing operation and low detection resolution.

In this paper, with the advantages of the LRF, i.e. strong adaptability to surroundings and high detection accuracy, two LRFs mounted on the cane robot are used as an alternative to obtain the gait data without wearable sensors. Thus, a mobile gait analysis system based on a cane robot and two LRFs is proposed.

However, two challenges remain for gait analysis and walking-ability evaluation using the proposed system.

1. It is difficult to obtain accurate 3D gait spatial-temporal parameters using LRFs that can only scan horizontal distance information.

2. The LRFs cannot directly detect the gait events including HS and TO, which makes it difficult to obtain the accurate gait cycle segmentation in gait analysis.

In this paper, a walking state classification algorithm based on HTSK fuzzy system is proposed to extract the accurate gait cycle. Since the plantar pressure system is the gold standard of gait event detection, the motion data for training HTSK fuzzy system is labeled by the walking states obtained from the plantar pressure system in the pre-experiments. The well-trained HTSK fuzzy system can then reliably classify the walking states using only the motion data obtained from LRFs. Moreover, the gait spatial-temporal parameters are extracted from the leg motion data segmented by the chronological walking state sequence. Based on the gait parameters of the clinical Tinetti scale, a quantitative walking-ability evaluation index is also proposed.

The main contributions are summarized as follows.

1. A gait detection method in daily walking environments without wearable sensors is proposed using a cane robot with two LRFs. Based on the proposed HTSK fuzzy system for walking state classification, the accuracy of recognizing different walking states by using only motion data from two LRFs reaches to 96.57%. The proposed gait parameter extraction algorithm achieves a low measuring error level (0.02 m (ME)

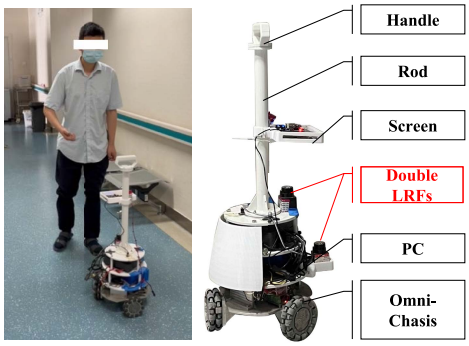


Fig. 1. The cane robot.

and 0.02 m (RMSE) of the step length, as well as 0.13 s (ME) and 1.23 s (RMSE) of the gait cycle).

2. In terms of the clinical Tinetti scale, an automatic walking-ability evaluation system is proposed. The walking-ability evaluation results are compared with the ratings given by the rehabilitation physician according to the Tinetti gait analysis scale.

3. The gait analysis and walking-ability evaluation system is built in the real world. Real experiments are conducted with healthy volunteers and patients.

The remainder of this paper is organized as follows. The cane robot, the overall concept of gait analysis and walking-ability evaluation system, and the human motion detection method are introduced in Section II-A. The gait analysis based on HTSK fuzzy system, the gait parameters extraction as well as the walking-ability evaluation are introduced in Section III. Pilot study and conclusions are presented in Section IV and Section V separately.

## II. Prototype of the Cane Robot With Two LRFs

### A. The Cane Robot System

In our previous study, a single LRF mounted cane-type omni-directional robot is designed for providing walking assistance and companionship based on the human-following control method [16].

In this paper, to ensure reliable gait analysis and rehabilitation evaluation under both the walking-aid and accompanying circumstances, two LRFs (URG-04LX-UG01, Hokuyo Automatic Co., Ltd.) are attached to the proposed cane robot and used to scan the environment in two horizontal planes, as shown in Fig. 1. The newly proposed cane robot system consists of three-wheel omni-directional mobile chassis, a 24V battery, a Personal Computer (PC), a metal rod, a 3D-printed handle, an emergency switch, and two LRFs.

As shown in Fig. 2, the cane robot collects the user's motion data with the two LRFs, estimates the user's walking intention, as well as analyzes the user's gait.

### B. Human Motion Detection With the Cane Robot

As shown in Fig. 4, the two LRFs scan the environment in two horizontal planes to detect the location of human shanks at different heights $z_0 = -42.0$ cm and $z_1 = -22.5$ cm. The Support Vector Domain Description (SVDD) based-method is introduced to extract the user's leg pair [17]. However, the leg detection method is hard to deal with the loose pants and long skirts. Elastic straps are used to restrain subjects' loose pants for reliable leg detection. $P_{l0}(x_{l0}, y_{l0}, z_0)$, and $P_{l1}(x_{l1}, y_{l1}, z_1)$ are the locations of the user's left shank detected by the LRFs, respectively. Similarly, the location of the user's right shank detected could be noted as $P_{r0}(x_{r0}, y_{r0}, z_0)$, and $P_{r1}(x_{r1}, y_{r1}, z_1)$ respectively. The line segments of $P_{l0}P_{l1}$ and $P_{r0}P_{r1}$ can be used to approximate the human legs.

The user's feet are estimated as two intersections (i.e. $P_{l2}(x_{l2}, y_{l2}, z_2)$, and $P_{r2}(x_{r2}, y_{r2}, z_2)$) of the line segments $P_{l0}P_{l1}$ and $P_{r0}P_{r1}$ with the ground, while $z_2 = 0.0$ cm. After the location of leg is mapped to the sagittal plane of the human body, as shown in Fig. 5, the location of the left foot $x_{l2}$ and the right foot $x_{r2}$ can be obtained by (1) based on the equal ratios theorem.

$$x_{l2} = \frac{z_0 x_{l1} - z_1 x_{l0}}{z_0 - z_1}, \quad x_{r2} = \frac{z_0 x_{r1} - z_1 x_{r0}}{z_0 - z_1}. \tag{1}$$

Similarly, as shown in Fig. 6 the locations in $Y^W$ axis can be determined by (2) in the coronal plane

$$y_{l2} = \frac{z_0 y_{l1} - z_1 y_{l0}}{z_0 - z_1}, \quad y_{r2} = \frac{z_0 y_{r1} - z_1 y_{r0}}{z_0 - z_1}. \tag{2}$$

The midpoint of the line connecting the leg ground contact point is recorded as the person's position $P_h(x_h, y_h, z_2)$, satisfying:

$$x_h = \frac{x_{l2} + x_{r2}}{2}, \quad y_h = \frac{y_{l2} + y_{r2}}{2}. \tag{3}$$

The human's posture is denoted as $\mathbf{q}_h = [x_h, y_h, \theta_h]^{\mathrm{T}}$. Human's orientation $\theta_h$ is defined as the person's positive facing direction, which can be estimated by the intention estimation algorithm proposed in [16].

The swing angles of the legs can be obtained in the sagittal and coronal planes of the human body, as shown in (4),

$$\begin{aligned} \alpha_{lx} &= \mathrm{atan2}(x_{l0} - x_{l1}, z_0 - z_1), \\ \alpha_{ly} &= \mathrm{atan2}(y_{l0} - y_{l1}, z_0 - z_1), \\ \alpha_{rx} &= \mathrm{atan2}(x_{r0} - x_{r1}, z_0 - z_1), \\ \alpha_{ry} &= \mathrm{atan2}(y_{r0} - y_{r1}, z_0 - z_1). \end{aligned} \tag{4}$$

According to the periodic characteristics of walking, the distance between legs changes periodically during walking and satisfies

$$d = \|\overrightarrow{P_{r2}P_{l2}}\|. \tag{5}$$

Based on the two LRFs, the positions of the left and right legs, human posture $\mathbf{q}_h$, speed $\dot{\mathbf{q}}_h = [\dot{x}_h, \dot{y}_h, \dot{\theta}_h]^{\mathrm{T}}$, acceleration $\ddot{\mathbf{q}}_h = [\ddot{x}_h, \ddot{y}_h, \ddot{\theta}_h]^{\mathrm{T}}$, swing angles of both legs in the sagittal and coronal plane $\alpha_{lx}$, $\alpha_{ly}$, $\alpha_{rx}$, $\alpha_{ry}$, and the distance between the legs $d$ can be estimated and used for gait analysis.

Moreover, as shown in Fig. 3, while the user holds the 3D-printed handle, the cane robot can provide the user with physical support. The force/torque sensor (WACOH TECH Inc.) is attached under the handle to record the interaction force $\mathbf{F}_h = [f_x \ f_y \ n_z]^{\mathrm{T}}$ between the human and the robot

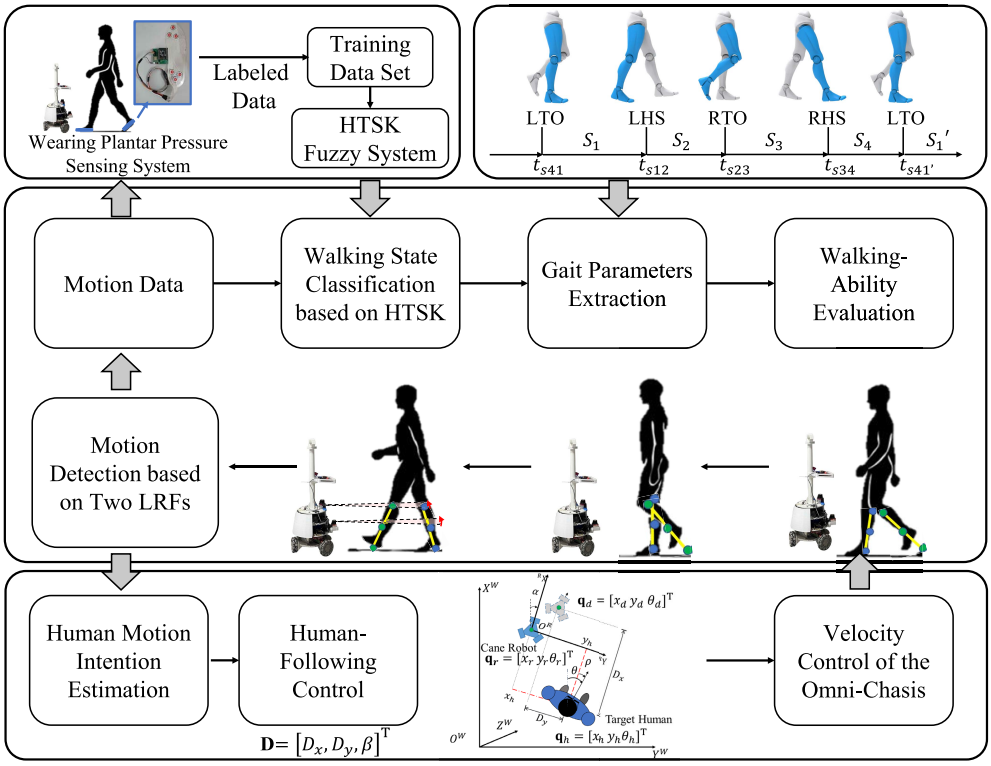


Fig. 2. The diagram of the gait analysis and evaluation system. Based on the human-following control method proposed in our former research [16], the cane robot can maintain a fixed relative posture $\mathbf{D} = [D_X, D_y, \beta]^{\mathrm{T}}$ with the target human, allowing the LRFs to obtain the accurate gait data. The fixed relative posture **D** can be customized under the rehabilitation physician's suggestion. Using only the motion data from LRFs, the HTSK fuzzy system can classify the walking states. The gait spatial-temporal parameters are then extracted based on the gait cycle segmented by walking states. The walking-ability evaluation system presents a quantitative results based on the obtained parameters.

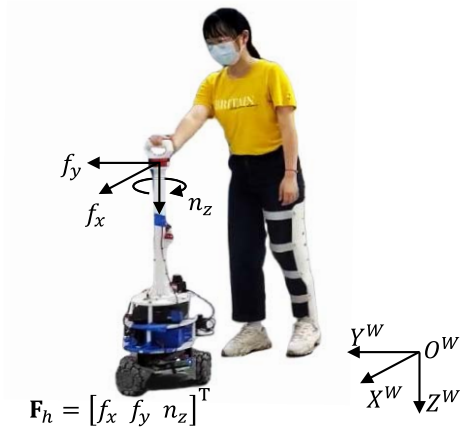


Fig. 3. The human-robot interaction force in the walking trial with physical support.

to identify whether the user uses aid or not in the walking-ability evaluation. $f_x$ and $f_y$ are the interaction forces in the $X^W$ axis and $Y^W$ axis, respectively. $n_z$ is the torque around the $Z^W$ axis.

### C. Walking States

The most widely used four gait phases of gait cycles (i.e. the swing phases of the left and right legs, the double support phases of the left and right legs) are studied in this paper [18], and the following five walking states are classified based on the TO and HS gait events, as shown in Fig. 2.

$S_0$: Static state.

$S_1$: The left leg is in the swing phase, while the right leg is in the support phase from $t_{s41}$ till $t_{s12}$.

$S_2$: Double support phase from $t_{s12}$ till $t_{s23}$, when the center of gravity shifts from right to left.

$S_3$: The left leg is in the support phase, while the right leg is in the swing phase from $t_{s23}$ till $t_{s34}$.

$S_4$: Double support phase from $t_{s34}$ till $t_{s41'}$, when the center of gravity shifts from left to right.

## III. Gait Analysis and Evaluation Algorithms Based on HTSK Fuzzy System

In this section, the gait analysis based on HTSK fuzzy system, the gait parameters extraction as well as the walking-ability evaluation are introduced. Although the conventional TSK fuzzy system [19] is widely applied in the classification, it usually uses distance-based approaches to compute membership grades. When the input dimensionality is high, the distances between data points become very similar [20]. Therefore, the saturation problem caused by softmax function makes it difficult for conventional TSK methods to solve the dimension disaster when dealing with the classification problem of high-dimensional data sets. In order to obtain accurate walking states for calculating gait parameters, a normalized firing level with data dimension introduced is pro-

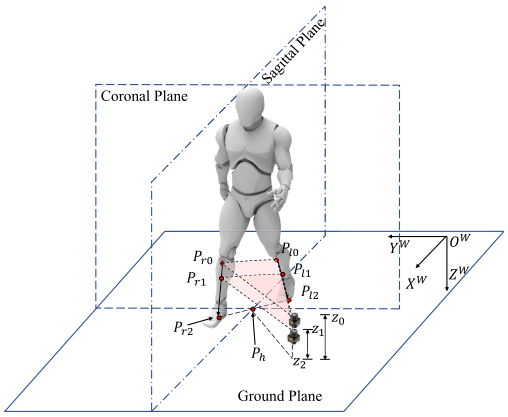


Fig. 4. Coordinate definition of gait analysis.

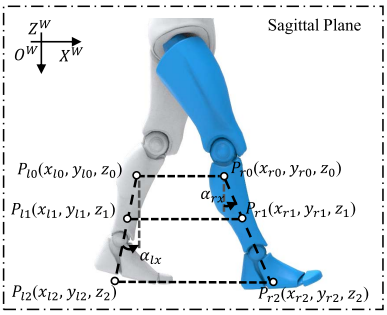


Fig. 5. Leg detection in sagittal plane.

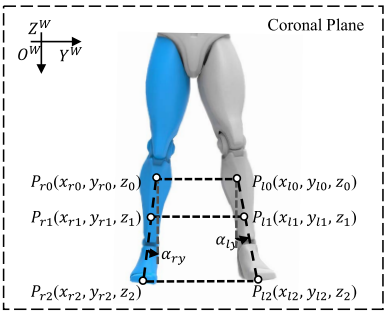


Fig. 6. Leg detection in coronal plane.

posed in HTSK fuzzy system, allowing the HTSK fuzzy system to handle high-dimensional data set during classifying the walking states based on the gait data obtained only by the LRFs.

## A. Preprocessing of Gait Data

The motion data set is denoted as $\mathcal{H} = \{\mathbf{h}_i\}_{i=1}^{N_0}$. $N_0$ is the number of samples. The collected data at time $t = i$ is denoted as $\mathbf{h}_i = \{h_1{}^{(i)}, h_2{}^{(i)}, \ldots, h_M{}^{(i)}\}$, $M$ is the dimension. $\mathbf{h}_i$ consists of the positions of both legs and the target human $\mathbf{x} = \{x_{l2}, x_{r2}, y_{l2}, y_{r2}, x_h, y_h\}$, the corresponding velocities $\dot{\mathbf{x}}$, the accelerations $\ddot{\mathbf{x}}$, the recorded motion angles of the shanks $\alpha_{lx}, \alpha_{ly}, \alpha_{rx}, \alpha_{ry}$ and corresponding angle velocities, the distance between the shanks $d$, as well as the gradient of the distance $\dot{d}$. $\mathcal{H}_S = \{\mathbf{h}_{si}\}_{i=1}^{N_0}$ is the motion data set standardized by $Z$-score transformation. The walking state at time $t = i$ is

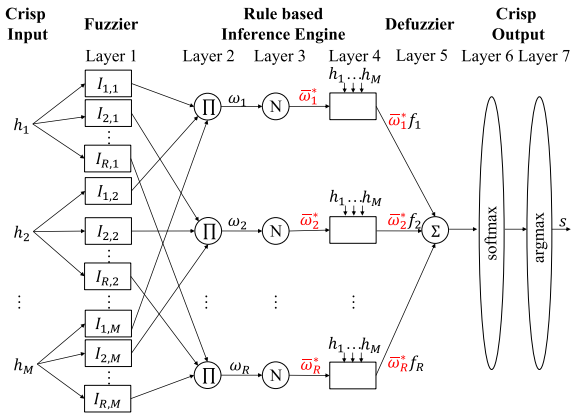


Fig. 7. The structure of HTSK fuzzy system.

denoted as $s_i$, $s_i \in \{S_0, S_1, S_2, S_3, S_4\}$. Consequently, the gait data set can be denoted as $\mathcal{M} = \{\mathbf{h}_i, s_i\}_{i=1}^{N_0}$. $N_0$ is the sample size of the data set.

## B. HTSK Fuzzy System for Walking State Classification

In the walking state classification problem, the training data set is denoted as $\mathcal{M}_T = \{\mathbf{h}_n, s_n\}_{n=1}^{N}$. $N$ is the size of the training set. $\mathbf{h}_n = \{h_1{}^{(n)}, h_2{}^{(n)}, \ldots, h_M{}^{(n)}\}$ is the $M$ dimensional feature vector of the $n$th sample. $s_n \in \{1, 2, \ldots, P\}$ is the label of the $P$-class data.

HTSK fuzzy system consists a set of If-Then rules, and the structure is shown in Fig. 7.

Suppose that an $M$-input single output HTSK fuzzy system has $R$ rules, and the $r$th rule is denoted as (6),

$$\begin{aligned} &\text{IF } h_1^{(n)} = I_{r,1}, h_2^{(n)} = I_{r,2}, \ldots, h_M^{(n)} = I_{r,M}, \\ &\text{THEN } f_r(\mathbf{h}_n) = \sum_{k=1}^{M} (h_m^{(n)} w_{r,m} + b_{r,0}). \end{aligned} \tag{6}$$

where $I_{r,m}$ $(r = 1, 2, \ldots, R; m = 1, 2, \ldots, M)$ is the membership degree function for the $m$th attributes after fuzzed in the $r$th rule. $w_{r,m}$ is the weight coefficient. $b_{r,0}$ is the bias coefficient.

Note that the output of each layer of HTSK fuzzy system is $O^j$, $j = 1, 2, \ldots, 7$. In the first two layers, the membership grade $O^1$, the firing level of each rule $O_r^2 = \omega_r$ are shown in (7). $c_{r,m}$ and $\sigma_{r,m}$ are the antecendent parameters.

$$O_{r,m}^1 = I_{r,m} = \exp(-\frac{(h_m - c_{r,m})^2}{2\sigma_{r,m}^2}), \omega_r = \prod_{m=1}^{M} I_{r,m}. \tag{7}$$

In the conventional TSK fuzzy system, the normalized firing level $\bar{\omega}_r$ is a typical softmax function (8), where $H_r = -\sum_{m=1}^{M}(\frac{(h_m - c_{r,m})^2}{2\sigma_{r,m}^2}) < 0$.

$$\bar{\omega}_r = \frac{\exp(H_r)}{\sum_{r=1}^{R} \exp(H_r)} \tag{8}$$

As the dimensionality $M$ increases, $H_r$ decreases, which leads to the saturation of softmax [21]. $\bar{\omega}_r$ tends to only give non-zero firing levels to the rule with maximum $H_r$

and thus results in a poor classification performance for high-dimensional input data sets.

In order to deal with the saturation problem, HTSK fuzzy system changes the normalized firing level $\bar{\omega}_r$ into $\bar{\omega}_r^*$ by replacing $H_r$ with its average $H_r^* = -\frac{1}{M}\sum_{m=1}^{M}(\frac{(h_m - c_{r,m})^2}{2\sigma_{r,m}^2})$, as shown in (9)

$$O_r^3 = \bar{\omega}_r^* = \frac{\exp(H_r^*)}{\sum_{r=1}^{R}\exp(H_r^*)}. \tag{9}$$

The scale of $H_r^*$ no longer depends on the dimensionality $M$. The saturation of softmax caused by the high-dimensional inputs is solved in a certain degree, and does not affect the firing levels any more. Therefore, the classification performance of HTSK for high-dimensional input data sets can be guaranteed.

The output of the HTSK fuzzy system, $s_n$, can be obtained by (10)-(12)

$$O_r^4 = \bar{\omega}_r^* f_r = \bar{\omega}_r^*(\sum_{m=1}^{M} h_m w_{r,m} + b_{r,0}). \tag{10}$$

$$O_p^5 = \sum_{r=1}^{R} O_r^4, \quad O_p^6 = \frac{\exp(O_p^5}{)}\sum_{p=1}^{P}\exp(O_p^5), \tag{11}$$

$$s_n = O^7 = \underset{p}{argmax}(O_p^6). \tag{12}$$

In this paper, we use $k$-means clustering to initialize the antecedent parameters $c_{r,m}$, and mini-batch gradient descent to optimize the parameters $b_{r,0}$, $w_{r,m}$, $c_{r,m}$ and $\sigma_{r,m}$ for training HTSK fuzzy system.

### C. Gait Parameters Extraction

As shown in Fig. 2, the switching moment of walking data sequence $S_1$-$S_2$-$S_3$-$S_4$-$S_1'$ can be denoted as $t_{s41}, t_{s12}, t_{s23}$ and $t_{s41'}$ respectively, and can be obtained based on the output walking states from HTSK fuzzy system. The gait parameters $\mathbf{u} = \{T, T_l, T_r, P_{LS}, P_{LD}, P_{RS}, P_{RD}, v, L_l, L_r, L_s, L_w, SI\}$ (concluded in [18]) can be obtained by applying the gait analysis algorithm based on HTSK (GAA-HTSK), as shown in Algorithm 1. $T$ is the gait cycle period. $T_l$ and $T_r$ are the step times of the left and right legs, respectively. The ratios of the swing phases are denoted as $P_{LS}$ and $P_{RS}$. $P_{LD}$ and $P_{RD}$ are the ratios of double support phases of the left and right legs, respectively. $v$ is the user's walking speed. $L_l$ and $L_r$ are the step lengths of left and right legs. $L_s$ is the stride lengths. $L_w$ is the step widths. $SI$ is the walking symmetry index of the step lengths [22].

### D. Walking-Ability Evaluation

In conformity with the conventional Tinetti gait analysis scale matching 12 points (See Appendix I), the corresponding algorithm is designed and the appropriate gait data variables and gait parameters are selected for the walking-ability evaluation.

**Algorithm 1** The GAA-HTSK

*

**Require:** The standardized motion data $\mathcal{H}_S = \{\mathbf{h}_{si}\}_{i=1}^{N_0}$, the well-trained HTSK

**Ensure:** The walking state $s_i$, the gait parameters $\mathbf{u}(j)$ of the $j$th gait cycle, the number of gait cycles $N_1$

```
Initialize j = 1, s_i, u(j), N_1
for i=1 to N_0 do
    Calculate s_i by h_si based on (6)-(7) and (9)-(12);
    if the jth state sequence S_1-S_2-S_3-S_4 is detected then
        Segment the gait cycle t_s41-t_s12-t_s23-t_s41';
        Calculate u(j) of the jth gait cycle [18], [22];
        N_1 = j;
        j = j + 1;
    end if
end for
return s_i, u(j), N_1
```

The walking-ability evaluation index can be denoted as $I$ satisfying

$$I = \sum_{i=0}^{5} a_i \tag{13}$$

where $a_i$ is the score of the each test in the scale, and can be obtained by the walking-ability evaluation algorithm (WAE), as shown in Algorithm 2.

Due to the limitation of engineering problems, Rule 1 and Rule 6 in the Tinetti gait analysis scale are not selected to design the corresponding evaluation indexes. However, by covering Rule 2, 3, 4, 5 and 7 in the Tinetti gait analysis scale, the walking-ability evaluation algorithm proposed in this paper can serves as an effective indication and reference for evaluating the walking ability in terms of left and right leg swing performance, whether the step length is equal, walking continuity, lateral deviation in the straight walking, whether there is external physical assistance and the walking posture. A maximum of 12 points is assigned to $I$. A higher score of $I$ indicates a better walking ability.

## IV. Pilot Study

Eleven subjects are involved in this study, as shown in Table I. There are seven healthy subjects (Subject 1∼4 and 8∼10) and four patients (Subject 5∼7 and 11). Subject 4, Subject 8, Subject 9 and Subject 10 wear a right lower limb holder (RLLH) or a left lower limb holder (LLLH) that locks unilateral knee movement to simulate a patient with lower limb dysfunction, as shown in Fig. 8. Four patients with right hemiplegia (RH, Subject 5), right leg ligament strain (RLLS, Subject 6), scoliosis (SCOL, Subject 7) and left ankle sprain wearing the lower limb holder (LASLLH, Subject 11) are also recruited. Subject 1∼7 participate the independent walking trials. Besides, Subject 8∼11 participate the walking trials with physical support.

Three kinds of experiments (i.e. walking state classification experiments, gait parameters analysis experiments, and

**Algorithm 2** The WAE

**Require:** The motion data set $\mathcal{H}$ with corresponding $N_1$ gait cycles, the interaction force $\mathbf{F}_h$ and gait parameters $\mathbf{u}$

**Ensure:** Walking-ability evaluation index $I$

Initialize $a_i$=0, $i$=0, 1,..., 5;

**if** [1] $\frac{1}{N_1}\sum_{j=1}^{N_1}(x_{r2}^{ts34}(j)-x_{l2}^{ts34}(j))>0$ **then** $a_0=2$;

**end if**

**if** [2] $\frac{1}{N_1}\sum_{j=1}^{N_1}(x_{l2}^{ts12}(j)-x_{r2}^{ts12}(j))>0$ **then** $a_1=2$;

**end if**

**if** [3] $|\frac{1}{N_1}\sum_{j=1}^{N_1}(L_l(j))-\frac{1}{N_1}\sum_{j=1}^{N_1}(L_r(j))|\le\Delta L$ **then** $a_2=2$;

**end if**

**if** [4] $\text{std}(v)\le\frac{1}{2N_1}\sum_{j=1}^{N_1}(v(j))$ **then** $a_3=2$;

**end if**

**if** [5] $|\max(y_h)|\le\Delta y_{min}$ **and** $\|\mathbf{F}_h\|_2\le\Delta F$ **then** $a_4=2$;

**else if** $\Delta y_{min}<|\max(y_h)|<\Delta y_{max}$ **or** $\|\mathbf{F}_h\|_2>\Delta F$ **then** $a_4=1$;

**end if**

**if** [6] $\frac{1}{N_1}\sum_{j=1}^{N_1}(L_w(j))\le\Delta L_{wmin}$ **then** $a_5=2$;

**else if** $\Delta L_{wmin}<\frac{1}{N_1}\sum_{j=1}^{N_1}(L_w(j))\le\Delta L_{wmax}$ **then** $a_5=1$;

**end if**

Calculate $I$ based on (13);

**return** $I$

The thresholds for the evaluation characteristics may vary from physician to physician, depending on their experience and attention to details [23]. In this algorithm, the thresholds are based on the rehabilitation physician's suggestions, including $\Delta L=5.0$ cm, $\Delta y_{max}=30.0$ cm, $\Delta y_{min}=10.0$ cm, $\Delta L_{wmax}=22.0$ cm, $\Delta L_{wmin}=11.5$ cm, and $\Delta F=10$ N.

[1] Rule 2a of the Tinetti gait analysis scale (See Table VI of Appendix I).

[2] Rule 2b of the Tinetti gait analysis scale.

[3] Rule 3 of the Tinetti gait analysis scale.

[4] Rule 4 of the Tinetti gait analysis scale.

[5] Rule 5 of the Tinetti gait analysis scale.

[6] Rule 7 of the Tinetti gait analysis scale.

walking-ability evaluation experiments) are conducted to validate the effectiveness of the proposed gait analysis and evaluation system. The ethics approval for experiments with subjects was granted by the Ethics Committee of Tongji Medical College, Huazhong University of Science and Technology (NO. IORG0003571). Written consents were obtained from all subjects.

### A. Walking State Classification Experiments

The walking state classification performances of the proposed HTSK fuzzy system and other five conventional machine learning classifier (i.e. Support Vector Machine (SVM), $k$-Nearest Neighbor ($k$-NN), Decision Tree (DT), Naive Bayesian (NB), and TSK) are compared.

TABLE I
THE INFORMATION OF SUBJECTS

| Subject | Gender | Age [year] | Weight [kg] | Height [cm] | Shoes Size [cm] | Health State | [1]Walking State |
|---|---|---|---|---|---|---|---|
| 1 | M | 25 | 58 | 168 | 26.0 | Normal | IW |
| 2 | M | 24 | 66 | 175 | 26.5 | Normal | IW |
| 3 | M | 24 | 56 | 162 | 26.5 | Normal | IW |
| 4 | M | 26 | 65 | 163 | 24.5 | RLLH | IW |
| 5 | M | 38 | 62 | 173 | 27.5 | RH | IW |
| 6 | F | 67 | 54 | 163 | 24.5 | RLLS | IW |
| 7 | M | 12 | 49 | 131 | 22.5 | SCOL | IW |
| 8 | M | 25 | 55 | 174 | 25.5 | LLLH | PS |
| 9 | M | 24 | 63 | 179 | 26.0 | RLLH | PS |
| 10 | F | 25 | 52 | 170 | 24.5 | RLLH | PS |
| 11 | F | 23 | 50 | 160 | 23.0 | LASLLH | PS |

[1] Walking State: Independent Walking (IW) and Physical Support (PS)

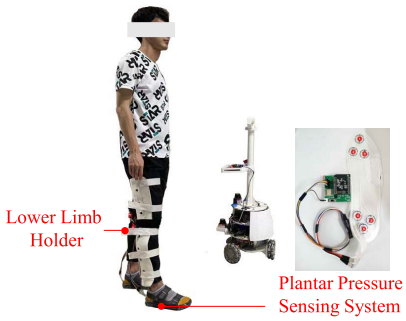


Fig. 8. Plantar pressure sensing system.

*1) Data Set Collection:* The gait data set $\mathcal{M}$ for training HTSK fuzzy system is collected in the pre-experiments. As mentioned in Section II and Section III, the motion data set $\mathcal{H}$ can be collected during the subject's walking. The plantar pressure sensing system is used as the gold standard of the walking states classification, and is only used to label the motion data set $\mathcal{H}$. As shown in Fig. 8, the plantar pressure sensing system consists of two groups of force-sensing resistors (FSRs) for detecting the plantar pressures, with six FSRs in each group. The threshold detection method is used to analyze the toe and heel motion data to obtain the classification of walking states [24]. Therefore, at time $t=i$, the walking state $s_i$ corresponding to the motion data $\mathbf{h}_i$ in the gait set $\mathcal{M}$ is labeled by the plantar pressure sensing system. The sample period of the proposed system is 100 ms.

*2) Procedures:* Wearing the plantar pressure sensing system, the subject stands behind the cane robot. Once the robot has initialized to maintain the relative fixed posture with the human, then the subject starts to walk 7.62 m (25 feet) forward at a self-selected speed, as shown in Fig. 9. The gait data set $\mathcal{M}_T$ of 11 subjects is obtained based on the data signals from two LRFs and the plantar pressure sensing system, including more than 30000 samples, multiple speeds (0.10∼0.73 m/s) and multiple step lengths (0.16∼1.03 m). Then, the HTSK fuzzy system and other five conventional machine learning classifiers (SVM, $k$-NN, DT, NB, and TSK) are trained and used to recognize the walking states using only the LRF motion data. For each method,


Fig. 9. The experimental environment in the union hospital.

TABLE II
AVERAGE PERFORMANCE OF WALKING STATE CLASSIFICATION

| | SVM | $k$-NN | DT | NB | TSK | HTSK |
|---|---|---|---|---|---|---|
| ACC [%] | 84.41 | 92.66 | 93.52 | 90.68 | 83.75 | **96.57** |
| STD [%] | 7.11 | 5.60 | 5.36 | 6.94 | 7.43 | **4.15** |
| F-Score [%] | 83.60 | 90.58 | 92.60 | 90.35 | 83.89 | **96.53** |

TABLE III
COMPARISON WITH SIMILAR RESEARCH LITERATURES

| Research | Sensor | Algorithm | States | ACC [%] |
|---|---|---|---|---|
| **Proposed** | LRFs | HTSK | 5 | **96.57** |
| [8] | FSRs | MRHMM | 6 | 83.21 |
| [9] | IMUs | CNN | 13 | 89.23 |
| [25] | EMG Sensors | SVM, C-SVC | 4 | 85.7 |
| [26] | Angular Sensors | MLP | 8 | 87.2∼94.5 |
| [27] | Encoder | FSM | 7 | >93.78 |

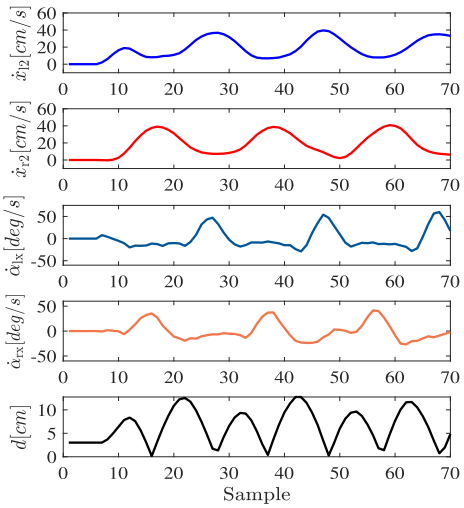


(a) The motion data

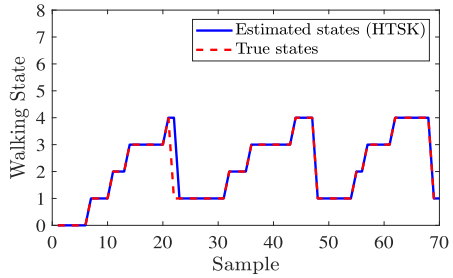


(b) Estimated walking states (HTSK) and reference states

Fig. 10. The gait data of Subject 1.

10-fold cross validation is used to evaluate the generalization ability.

*3) Setting of Walking State Classification Algorithms:*

1) SVM: The linear kernel function is adopted in SVM. The penalty coefficient is set to 40, and other parameters are the default values.
2) $k$-NN: The number of nearest neighbors is 5, and other parameters are set to the default value.
3) DT: The default algorithm and parameters in sklearn library are used.
4) NB: Gaussian naive Bayesian model is used in NB, and other parameters are selected by default in sklearn library.
5) TSK: According to the actual experimental experience, the number of fuzzy rules is set to 60. The mini-batch gradient descent and Adam optimizer are used for optimization. The selected learning rate is 0.01. The batch size is set to 32. Randomly select 10% of the data from the training set as the validation set for early-stopping to prevent overfitting.
6) HTSK: All the settings are the same with those of TSK fuzzy system.

The widely accepted accuracy is adopted as the performance evaluation criteria. The definition of accuracy is:

$$\mathrm{ACC} = \frac{T_P + T_N}{T_P + T_N + F_P + F_N}, \tag{14}$$

where $T_P$, $T_N$, $F_P$, and $F_N$ represent the number of true positive, false negative, false positive and true negative samples.

*4) Walking State Classification Performance:* Typical walking state classification results for three gait cycles are shown in Fig. 10. The motion data of Subject 1 is shown in Fig. 10a. The walking states estimated by the HTSK fuzzy system and the true walking states obtained by the plantar pressure sensing system are shown in Fig. 10b.

The results of the walking state classification accuracy are shown in Table II. Among them, the accuracy of the proposed HTSK fuzzy system is the highest, up to 96.57%, which is improved more than 10%, compared with the performance of TSK fuzzy system. As shown in Table III, compared with other similar research literature work, the proposed system performs well and achieves a higher accuracy. The results reveal that the HTSK-based walking analysis system can effectively identify the walking states.

## B. Gait Parameters Analysis Experiments

The extracted gait parameters of the eleven subjects are shown in Table IV. The left and right swing phases of Subject 1∼3 are evenly distributed. Meanwhile, their mean values of the walking symmetry index $SI$ are small, indicating that their legs swing symmetrically during walking. Compared with the healthy subjects, the symmetry indexes $SI$ of Subject 4∼11 have larger absolute values, which means that the legs of Subject 4∼11 cannot move symmetrically.

For assessing the accuracy of extracting gait parameters, the mean error (ME) and the root mean square error (RMSE) between the gait parameters extracted by the proposed system and true values should be calculated.

TABLE IV
RESULTS OF GAIT PARAMETERS

| Gait Parameters | Subject 1 | Subject 2 | Subject 3 | Subject 4 | Subject 5 | Subject 6 | Subject 7 | Subject 8 | Subject 9 | Subject 10 | Subject 11 |
|---|---|---|---|---|---|---|---|---|---|---|---|
| Gait Cycles | 6 | 5 | 6 | 5 | 4 | 5 | 5 | 5 | 6 | 5 | 6 |
| $T$ [s] | 2.07 ± 0.09 | 2.35±0.21 | 1.22±0.44 | 1.96±0.11 | 0.97±0.85 | 2.00±1.55 | 1.17±0.20 | 1.47±0.13 | 1.76±0.75 | 1.27±0.45 | 1.44±0.09 |
| $T_l$ [s] | 1.05±0.05 | 1.22±0.72 | 0.69±0.46 | 1.07±0.10 | 1.30±1.34 | 1.92±1.54 | 0.58±0.20 | 0.71±0.13 | 1.17±0.09 | 0.94±0.09 | 0.68±0.10 |
| $T_r$ [s] | 1.02±0.07 | 1.10±0.17 | 0.55±0.12 | 0.90±0.08 | 0.70±0.67 | 1.03±0.68 | 0.58±0.15 | 0.75±0.08 | 0.78±0.35 | 0.68±0.44 | 0.76±0.05 |
| $P_{LS}$ [%] | 32.30±5.72 | 34.54±2.72 | 45.95±8.36 | 31.48±2.22 | 17.24±1.13 | 5.13 ±12.47 | 15.81±6.32 | 36.25±2.61 | 41.18±4.64 | 25.05±3.07 | 33.97±2.62 |
| $P_{LD}$ [%] | 19.75±7.79 | 12.12±6.04 | 16.20±4.63 | 17.08±2.05 | 43.10±7.34 | 34.51±9.67 | 39.03±9.17 | 13.36±5.42 | 17.65±2.56 | 28.75±3.55 | 16.25±5.27 |
| $P_{RS}$ [%] | 32.51±8.41 | 33.15±4.55 | 43.21±8.25 | 27.60± 4.20 | 37.93±9.72 | 46.15±10.83 | 19.35±5.56 | 46.13±4.32 | 29.41±7.28 | 36.47±6.86 | 44.52±5.23 |
| $P_{RD}$ [%] | 14.69±9.43 | 20.18±5.65 | 17.64±3.72 | 23.84±2.66 | 16.94±8.52 | 27.27 ±7.28 | 44.81±8.87 | 12.70±2.03 | 11.76±6.81 | 17.23±7.09 | 15.70±2.80 |
| $v$ [m/s] | 0.20±0.06 | 0.13±0.03 | 0.28±0.06 | 0.14±0.06 | 0.11±0.07 | 0.12±0.08 | 0.18±0.06 | 0.25±0.48 | 0.19±0.03 | 0.19±0.07 | 0.26±0.02 |
| $L_l$ [m] | 0.34±0.03 | 0.37±0.11 | 0.45±0.27 | 0.36±0.06 | 0.25±0.35 | 0.33±0.04 | 0.43±0.26 | 0.36±0.12 | 0.32±0.01 | 0.46±0.04 | 0.29±0.04 |
| $L_r$ [m] | 0.34±0.03 | 0.38±0.11 | 0.41±0.17 | 0.32±0.03 | 0.08±0.19 | 0.18±0.25 | 0.59±0.12 | 0.32±0.07 | 0.36±0.02 | 0.17±0.22 | 0.33±0.12 |
| $L_s$ [m] | 0.50±0.18 | 0.60±0.21 | 0.61±0.11 | 0.52±0.18 | 0.16±0.33 | 0.34±0.34 | 0.77±0.26 | 0.55±0.18 | 0.47±0.18 | 0.39±0.37 | 0.50±0.19 |
| $L_w$ [m] | 0.18±0.01 | 0.18±0.01 | 0.13±0.01 | 0.19±0.01 | 0.21±0.02 | 0.19±0.02 | 0.12±0.01 | 0.16±0.04 | 0.22±0.01 | 0.18±0.01 | 0.17±0.07 |
| $SI$ [%] | 0.53±2.36 | 2.93±1.04 | 8.11±6.60 | -12.77±8.75 | -50.62±41.20 | -59.63±18.51 | -31.83±41.83 | 23.95±3.46 | -6.43±1.88 | -8.04±12.84 | 11.65±8.49 |

With the low latency (8.3 ms) and high resolution (1280 × 1024) of motion tracking, the vision-based motion capture system OptiTrack (Flex 13 Series, NaturalPoint, Inc.) has become a widely accepted gold standard for gait analysis. The markers are set on the lateral crural region of knee joints, shanks, toes, and heels to obtain the subject's motion data, as shown in Fig. 11. Gait parameters obtained from the 3D motion measurements of the markers in the motion capture system are used as true values of gait parameters.

*1) Procedures:* Wearing the reflective markers, the healthy subject stands behind the cane robot. Once the robot has initialized to maintain the relative fixed posture with the human, then the subject starts to walk forward. After the subject completes the walking trial, the gait data set $\mathcal{M}$ is obtained by the proposed system. Then, the gait parameters can be obtained by Algorithm 1.

*2) Gait Parameter Errors:* Results of errors (ME, RMSE) and standard deviation (STD) of the gait variables for the healthy subjects are shown in Table V. The errors of step length are 0.02 m (ME) and 0.02 m (RMSE) respectively. The gait cycle errors are 0.13 s (ME) and 1.23 s (RMSE), respectively. It shows that the proposed system is at a low measuring error level.

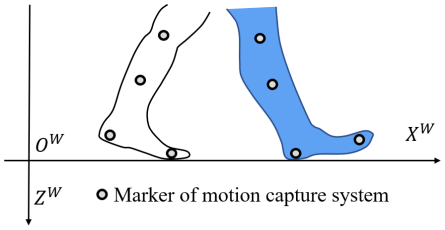


Fig. 11. The configuration of OptiTrack markers.

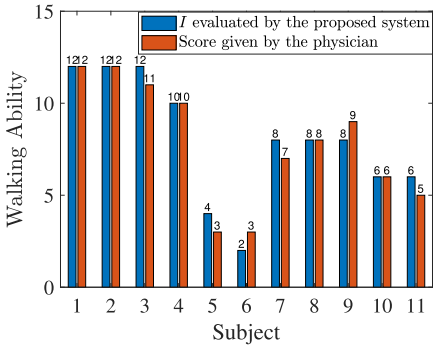


Fig. 12. Results of walking-ability evaluation.

## C. Walking-Ability Evaluation Results

In order to reduce the influence of human factors on the error caused by different physicians' evaluations and maintain the homogeneity of evaluation results, the attending physician of the Department of Rehabilitation Medicine is invited to participate in the walking-ability evaluation. According to the Tinetti scale, the walking ability of each subject is evaluated only once by score based on the recorded video of the walking trial. The walking-ability evaluation results evaluated by the Algorithm 2 and the scores given by the physician based on the Tinetti gait analysis scale are shown in Fig. 12. The x-axis indicates the eleven subjects. The y-axis indicates the walking-ability evaluation results.

The walking-ability evaluation index of healthy subjects (Subject 1, Subject 2, and Subject 3) are significantly higher than that of the other eight subjects with lower limb dysfunction, indicating that the walking ability of healthy subjects are better than other subjects. Moreover, the results evaluated by the proposed system and scored by the physician based on Tinetti gait assessment tool are similar, indicating that the proposed walking-ability evaluation index and the cane robot based system can effectively evaluate the walking ability.

## D. Discussion

In this study, a novel mobile gait analysis and evaluation system based on a cane robot is proposed and validated. HTSK fuzzy system is also proposed for recognizing different walking states by using only motion data from two LRFs. Comparing with existing gait analysis studies [6], [7], [8], [9]

TABLE V
RESULTS OF GAIT PARAMETER ERRORS

| Gait Parameters | ME±STD | RMSE |
|---|---|---|
| $T$ [s] | 0.13±0.11 | 1.23 |
| $T_l$ [s] | 0.13±0.09 | 0.84 |
| $T_r$ [s] | 0.12±0.12 | 0.75 |
| $P_{LS}$ [%] | 4.69±4.43 | 3.17 |
| $P_{LD}$ [%] | 2.27±1.63 | 6.94 |
| $P_{RS}$ [%] | 2.54±2.21 | 3.11 |
| $P_{RD}$ [%] | 6.33±4.71 | 2.40 |
| $v$ [m/s] | 0.01±0.01 | 0.03 |
| $L_l$ [m] | 0.02±0.01 | 0.02 |
| $L_r$ [m] | 0.02±0.01 | 0.02 |
| $L_s$ [m] | 0.02±0.01 | 0.02 |
| $L_w$ [m] | 0.02±0.01 | 0.02 |
| $SI$ [%] | 5.46±3.21 | 3.19 |

based on motion capture systems, wearable sensors or vision sensors for gait detection, the proposed system has attractive features, including no wearable sensors needed, low-cost, high mobility. Even only using the motion data obtained by LRFs, the proposed HTSK fuzzy system reaches to the accuracy of 96.57%. which is improved more than 10%, compared with the performance of TSK fuzzy system in Table II. Although the accuracy of some gait analysis studies based on plantar pressure sensors and IMUs can reach 100% [28], the accuracy of the proposed system is at a similar level to most of the current gait analysis studies (85.21% to 94.5% accuracy), as shown in Table III.

The proposed gait parameter extraction algorithm performs well in this study, and achieves a low measuring error (0.02 m (ME) and 0.02 m (RMSE) of the step length) compared with the previous study [29]. Moreover, since all the subjects walk at their self-selected speeds in this study, there are speeding up, slowing down and even pauses in the process of walking forward. Therefore, the standard deviations of the extracted speeds are larger than those of volunteers' walking at a constant speed on the treadmill in previous studies [10].

The small difference between the scores calculated from the proposed method and the scores performed by the rehabilitation physician may due to the error of observation and different attention to details between the proposed system and the physician, which is clinically acceptable. Many studies have verified that even different physicians may rate the same subject differently due to their different experience and attention to details while using the same gait analysis scale [23]. Thus, quantitative gait analysis can help physicians accurately and reliably assess patients' walking ability. As shown in Fig. 12, the walking-ability evaluation results evaluated by the proposed system and the physician are similar. Although less kinematic information was used for calculating the walking-ability evaluation index, the proposed system is a valuable tool as its more convenience, lower cost and less site restriction compared with the motion capture system or IMUs based wearable system. The spatial-temporal parameters obtained in this study have been applied in clinical gait analysis. This would be beneficial in the situations of tracking the progress of gait after patients can walk independently.

There are also some limitations in this study. First, the proposed leg detection method is hard to deal with the loose pants and long skirts. Second, the influence of sampling rate of the LRF on this system is considered and still needs to be investigated for further improving the accuracy. Third, due to the differences in walking patterns between patients and healthy subjects, it has to collect the patients' training data sets for recognizing walking states. Fourth, the small size of the subject group might influence the validity of the walking-ability evaluation. Fifth, since the subjects' walking speeds during the walking trials are self-selected speeds and vary over time, it is not applicable for analyzing the precise relationship between the accuracy of the proposed method, the walking speed, and the stride length in this paper. Finally, it is also difficult to correlate the low walking ability with a particular pathology. This is helpful for understanding the capacity of the proposed system on clinical diagnosis, and for further improvement on the walking-ability evaluation index.

TABLE VI
TINETTI GAIT ASSESSMENT TOOL

| Domain | Evaluation Rules |
|---|---|
| 1. Indication of gait | Any hesitancy or multiple attempts = 0<br>No hesitancy = 1 |
| 2.Step length and height | a. Right foot swings<br>Does not pass the left stance foot = 0<br>Steps past the left foot = 1<br>Does not clear floor = 0<br>Clears floor = 1<br>b. Left foot swings<br>Does not pass the right stance foot = 0<br>Steps past the right foot = 1<br>Does not clear floor = 0<br>Clears floor = 1 |
| 3. Step symmetry | Right and left step length not equal = 0<br>Right and left step length equal = 1 |
| 4. Step continuity | Stopping or discontinuity between steps = 0<br>Steps continuous = 1 |
| 5. Path | Marked deviation = 0<br>Mild/moderate deviation or uses aid = 1<br>Straight without aid = 2 |
| 6. Trunk | Marked sway or uses aid = 0<br>No sway but flexed knees or back or spread arms wide = 1<br>No sway, flexion, widened arms or aid = 2 |
| 7. Walking stance | Heels apart = 0<br>Heels almost touching while walking = 1 |

## V. CONCLUSION

In this study, a novel mobile gait analysis and evaluation system based on a cane robot is proposed and validated. Eleven subjects are involved in the experiments. The proposed HTSK fuzzy system achieve the 96.57% accuracy of recognizing different walking states by using only motion data from two LRFs. GAA-HTSK and WAE algorithms perform well in this study. The approach has great potential for further applications on intelligent diagnosis, healthcare automation and robotics-assisted rehabilitation using the cane robot or a mobile robot in both the cases of walking-aid and accompanying during independent walking.

Future work would be focusing on transfer learning method for generalizing the suitable walking states classifier with less collection of the patients' training data sets and improve the classification accuracy.

## APPENDIX I

See Table VI.

## REFERENCES


[1] D. Jarchi, J. Pope, T. K. M. Lee, L. Tamjidi, A. Mirzaei, and S. Sanei, "A review on accelerometry-based gait analysis and emerging clinical applications," *IEEE Rev. Biomed. Eng.*, vol. 11, pp. 177–194, 2018.

[2] A. D. Kloos, N. E. Fritz, S. K. Kostyk, G. S. Young, and D. A. Kegelmeyer, "Clinimetric properties of the Tinetti mobility test, four square step test, activities-specific balance confidence scale, and spatiotemporal gait measures in individuals with Huntington's disease," *Gait Posture*, vol. 40, no. 4, pp. 647–651, Sep. 2014.

[3] M. K. Holden, K. M. Gill, and M. R. Magliozzi, "Gait assessment for neurologically impaired patients: Standards for outcome assessment," *Phys. Therapy*, vol. 66, no. 10, pp. 1530–1539, Dec. 1986.

[4] H. F. Maqbool, M. A. B. Husman, M. I. Awad, A. Abouhossein, N. Iqbal, and A. A. Dehghani-Sanij, "A real-time gait event detection for lower limb prosthesis control and evaluation," *IEEE Trans. Neural Syst. Rehabil. Eng.*, vol. 25, no. 9, pp. 1500–1509, Sep. 2017.

[5] S. Ding, X. Ouyang, T. Liu, Z. Li, and H. Yang, "Gait event detection of a lower extremity exoskeleton robot by an intelligent IMU," *IEEE Sensors J.*, vol. 18, no. 23, pp. 9728–9735, Dec. 2018.

[6] B. Carse, B. Meadows, R. Bowers, and P. Rowe, "Affordable clinical gait analysis: An assessment of the marker tracking accuracy of a new low-cost optical 3D motion analysis system," *Physiotherapy*, vol. 99, no. 4, pp. 347–351, Dec. 2013.

[7] A. Pfister, A. M. West, S. Bronner, and J. A. Noah, "Comparative abilities of Microsoft Kinect and Vicon 3D motion capture for gait analysis," *J. Med. Eng. Technol.*, vol. 38, no. 5, pp. 274–280, 2014.

[8] F. Attal, Y. Amirat, A. Chibani, and S. Mohammed, "Automatic recognition of gait phases using a multiple-regression hidden Markov model," *IEEE/ASME Trans. Mechatronics*, vol. 23, no. 4, pp. 1597–1607, Aug. 2018.

[9] B.-Y. Su, J. Wang, S.-Q. Liu, M. Sheng, J. Jiang, and K. Xiang, "A CNN-based method for intent recognition using inertial measurement units and intelligent lower limb prosthesis," *IEEE Trans. Neural Syst. Rehabil. Eng.*, vol. 27, no. 5, pp. 1032–1042, May 2019.

[10] L. Wang, Y. Sun, Q. Li, T. Liu, and J. Yi, "IMU-based gait normalcy index calculation for clinical evaluation of impaired gait," *IEEE J. Biomed. Health Informat.*, vol. 25, no. 1, pp. 3–12, Jan. 2021.

[11] J. S. Park, C. M. Lee, S.-M. Koo, and C. H. Kim, "Gait phase detection using force sensing resistors," *IEEE Sensors J.*, vol. 20, no. 12, pp. 6516–6523, Jun. 2020.

[12] Z. Qaiser, A. Faraz, and S. Johnson, "Feasibility study of a rapid evaluate and adjust device (READ) for custom foot orthoses prescription," *IEEE Trans. Neural Syst. Rehabil. Eng.*, vol. 28, no. 8, pp. 1760–1770, Aug. 2020.

[13] J. A. Ramirez-Bautista, J. A. Huerta-Ruelas, S. L. Chaparro-Cárdenas, and A. Hernández-Zavala, "A review in detection and monitoring gait disorders using in-shoe plantar measurement systems," *IEEE Rev. Biomed. Eng.*, vol. 10, pp. 299–309, 2017.

[14] W. Chi, J. Wang, and M. Q.-H. Meng, "A gait recognition method for human following in service robots," *IEEE Trans. Syst., Man, Cybern., Syst.*, vol. 48, no. 9, pp. 1429–1440, Sep. 2018.

[15] J. Paulo, P. Peixoto, and U. J. Nunes, "ISR-AIWALKER: Robotic Walker for intuitive and safe mobility assistance and gait analysis," *IEEE Trans. Human-Mach. Syst.*, vol. 47, no. 6, pp. 1110–1122, Dec. 2017.

[16] Q. Yan, J. Huang, Z. Yang, Y. Hasegawa, and T. Fukuda, "Human-following control of cane-type walking-aid robot within fixed relative posture," *IEEE/ASME Trans. Mechatronics*, vol. 27, no. 1, pp. 537–548, Feb. 2022.

[17] W. Chung, H. Kim, Y. Yoo, C.-B. Moon, and J. Park, "The detection and following of human legs through inductive approaches for a mobile robot with a single laser range finder," *IEEE Trans. Ind. Electron.*, vol. 59, no. 8, pp. 3156–3166, Aug. 2012.

[18] M. W. Whittle, *Gait Analysis: An Introduction*. Oxford, U.K.: Butterworth, 2014.

[19] T. Takagi and M. Sugeno, "Fuzzy identification of systems and its applications to modeling and control," *IEEE Trans. Syst., Man, Cybern.*, vol. SMC-15, no. 1, pp. 116–132, Jan. 1985.

[20] M. E. Houle, H.-P. Kriegel, P. Kröger, E. Schubert, and A. Zimek, "Can shared-neighbor distances defeat the curse of dimensionality?" in *Proc. Int. Conf. Sci. Stat. Database Manag.* Berlin, Germany: Springer, 2010, pp. 482–500.

[21] Y. Wen, Z. Li, and Y. Qiao, "Noisy softmax: Improving the generalization ability of DCNN via postponing the early softmax saturation," in *Proc. IEEE Conf. Comput. Vis. Pattern Recognit. (CVPR)*, Jun. 2017, pp. 4021–4030.

[22] E. Kodesh, M. Kafri, G. Dar, and R. Dickstein, "Walking speed, unilateral leg loading, and step symmetry in young adults," *Gait Posture*, vol. 35, no. 1, pp. 66–69, Jan. 2012.

[23] A. D. Kloos et al., "Interrater and intrarater reliability of the Tinetti balance test for individuals with amyotrophic lateral sclerosis," *J. Neurolog. Phys. Therapy*, vol. 28, no. 1, pp. 12–19, 2004.

[24] R. Luo, S. Sun, X. Zhang, Z. Tang, and W. Wang, "A low-cost end-to-end sEMG-based gait sub-phase recognition system," *IEEE Trans. Neural Syst. Rehabil. Eng.*, vol. 28, no. 1, pp. 267–276, Jan. 2020.

[25] H. Huang, F. Zhang, L. J. Hargrove, Z. Dou, D. R. Rogers, and K. B. Englehart, "Continuous locomotion-mode identification for prosthetic legs based on neuromuscular–mechanical fusion," *IEEE Trans. Biomed. Eng.*, vol. 58, no. 10, pp. 2867–2875, Oct. 2011.

[26] D.-X. Liu, X. Wu, W. Du, C. Wang, and T. Xu, "Gait phase recognition for lower-limb exoskeleton with only joint angular sensors," *Sensors*, vol. 16, no. 10, pp. 1579–1600, 2016.

[27] F. Zhang, M. Liu, and H. Huang, "Effects of locomotion mode recognition errors on volitional control of powered above-knee prostheses," *IEEE Trans. Neural Syst. Rehabil. Eng.*, vol. 23, no. 1, pp. 64–72, Jan. 2015.

[28] H. T. T. Vu et al., "A review of gait phase detection algorithms for lower limb prostheses," *Sensors*, vol. 20, no. 14, pp. 3972–3992, 2020.

[29] M. Zago et al., "Gait evaluation using inertial measurement units in subjects with Parkinson's disease," *J. Electromyogr. Kinesiol.*, vol. 42, pp. 44–48, Oct. 2018.